Measurement 165 (2020) 108184

Contents lists available at ScienceDirect

Measurement

journal homepage: www.elsevier.com/locate/measurement

Foot type classification using sensor-enabled footwear and 1D-CNN

Zhanyong Mei [a], Kamen Ivanov [b,c], Guoru Zhao [b], Yuanyuan Wu [a], Mingzhe Liu [a], Lei Wang [b,*]

[a] College of Cyber Security, Chengdu University of Technology, Chengdu 610059, China
[b] Shenzhen Institutes of Advanced Technology, Chinese Academy of Sciences, Shenzhen 518055, China
[c] Shenzhen College of Advanced Technology, University of Chinese Academy of Sciences, Shenzhen 518055, China

ARTICLE INFO

Article history:
Received 30 March 2020
Received in revised form 30 June 2020
Accepted 2 July 2020
Available online 6 July 2020

Keywords:
Foot type classification
Sensor insole
1D CNN
Inertial sensor
Force sensor

ABSTRACT

Poor selection of footwear, underestimation of foot health, sedentary life, and lack of accessible foot screening can have significant long-term adverse effects on the health of lower limbs. Unobtrusive, pervasive methods for automated foot screening have the potential to allow for timely detection of foot abnormalities. In the present study, we describe a proof-of-concept where data collected through sensor-enabled insoles and processed through one-dimensional convolutional neural networks were used to distinguish normal, cavus, and planus feet. We explored several combinations of sensor modalities to find the one that reflects foot types optimally. The highest accuracy of classification of 99.26% was achieved when angular velocity and force sensing were combined. Based on results, we suggest that sensor insoles, combined with optimal classification techniques, could be used for foot screening.

1. Introduction

According to the structure of the foot arch, there are three types of feet: normal, planus, and cavus foot. The planus foot exhibits a wholly or partly collapsed arch, whereas cavus foot characterizes with a high longitudinal arch. Both of these abnormal foot types are highly prevalent. The proportion of the population with flat feet is about 2.2% among all age groups [1]. The low arch foot is found in 10.3% of the population in the age range 7–14 [2]. The prevalence of cavus foot is about 10.5% in the age group 16–65 years [3]. Due to the gait alteration that occurs as a result of these foot deformities, they are also associated with a higher incidence of lower limb injuries and increased risk for the development of medial tibial stress syndrome and patellofemoral pain [4]. Individuals with cavus foot may have unstable gait, ankle sprains, or pain in the metatarsal heads [6]. With the progression of the cavus foot condition, surgery will be necessary [5]. In the case of inappropriately selected shoes or foot orthotics, the condition of feet and ankles will worsen [7].

Determining foot status requires morphological measurement, which typically involves anthropometric methods, visual inspection, footprint measurement, and radiographic evaluation [8]. When applying such techniques, the validity of the measurement heavily depends on the experience of the podiatrist or orthopedist. Also, despite its diagnostic value, X-ray imaging of the foot is not appropriate for screening due to the associated radiation exposure. Specialized systems for gait analysis, such as force plates [9], plantar pressure platforms [10], and motion capturing systems using a camera and optical makers [11], allow for accurate classification or clustering of the foot types. For instance, a camera-based Vicon MX Motion Capture System was used to evaluate the effect of foot orthoses for the correction of flexible flat foot [12]. The 3D foot shape, acquired using a 3D laser scanner, can also indicate the location and severity of abnormal foot regions [13].

However, these are stationary systems confined to use in laboratory settings and not being suitable for mass foot screening and long-term monitoring. Therefore, new types of devices are needed to serve such purposes. Our primary concern behind conducting this research was to design and validate a method for unobtrusive screening and monitoring of foot function based on a sensor-enabled insole. In the current study, we integrated inertial sensor and force sensors into an insole. In this design, the inertial sensor allows acquiring the kinematic information, and the force sensors capture the kinetic information. The fusion of those two kinds of information allows reflecting the motion characteristics of each foot type entirely. Besides, our design involves wearable system technology. It thus facilitates experiments outside laboratories, in natural daily life settings, that are very close to the real conditions of mass screening of the foot types.

Gait analysis takes place for analysis of locomotion ability, clinical evaluation, and monitoring of the daily activities of the patients [14]. For the sensing, force sensors, and inertial sensors incorporating accelerometer and gyroscope are typically used.

* Corresponding author.
E-mail address: wang.lei@siat.ac.cn (L. Wang).

https://doi.org/10.1016/j.measurement.2020.108184
0263-2241/

Features can be explicitly defined, i.e., handcrafted, or, when using the latest machine learning approaches, be automatically determined. While conventional machine learning methods heavily depend on the handcrafted features, the latter might not reflect essential characteristics appropriately and thus lead to bias and lower the performance of the classifier. Recently, one-dimensional convolutional neural networks (1D CNN) have gained popularity for their unprecedented ability to extract discriminative features from raw data automatically. They have successfully been applied for human activity recognition [15], extraction of gait parameters [16], and classification of gait type [18]. In the present study, we hypothesized that during the foot motion, each foot type exhibits characteristic "marks" in the sensor signals. To explore the validity of this assumption empirically, we developed a full wearable gait analysis framework. It involves a multi-modal sensor insole for signal collection and a set of 1D-CNNs neural networks for automatic classification of foot types. Our aims were:

(1) To prove whether our designed sensor insole could serve foot type classification.
(2) To construct 1D-CNNs, optimize the network parameters, and compare the performance of the classifiers constructed using individual modalities and combinations of sensor data.
(3) Based on the performance comparison, to determine the optimal sensor configuration that would allow for a high accuracy while using a lower volume of gait data.
(4) To challenge the benefits of deep learning methods for foot type classification by comparing them with conventional machine learning methods.

The rest of this work is organized as follows: In Section 2, the related works on foot type evaluation and classification are introduced. Section 3 provides information about the design of the custom smart insole and the acquisition of experimental data. The algorithms used in this work are described in Section 4. In Section 5, the results of the algorithms and performance comparison are presented. Discussion and conclusion are given in Sections 6 and Section 7, respectively.

2. Related work

Each foot type is associated with a specific locomotion pattern. The exploration of the motion characteristics of each foot type allows building methods for automatic recognition of the foot type. Technically, the data required for such analyses are obtained through plantar pressure measurement systems, force plates, and optoelectronic motion capture systems.

Based on a plantar pressure measurement system emed®-x 400, Buldt et al. [19] found that the lowest average and minimum center of pressure (CoP) velocity during the terminal stance phase were lower in cavus foot compared to planus foot. Cavus foot had the highest maximum CoP velocity during the pre-swing stance [19]. The planus foot had the smallest index range of lateral-medial force during the terminal phase [19]. Among normal foot, planus foot and cavus foot, the cavus foot exhibited the highest center of pressure excursion index (CPEI); the planus foot showed the smallest CPEI values, and the normal foot exhibited the lowest peak pressure [17]. The peak pressures under the fourth and fifth metatarsophalangeal joints of the planus foot are lower than the ones of normal foot and cavus foot [29]. In previous studies, the stability of planus and normal feet was evaluated based on kinetic data from force plates. The force under the first hallux of pes planus is higher than that of normal foot [23]. In that, significant differences were found upon quantification through sample entropy [21], CoP velocity, and total velocity [22]. Based on measurements with an insole pressure system Pedar-X, it was determined that the contact area in the medial midfoot, as well as the maximum force and peak pressure in the lateral forefoot, are different between the normal foot and planus foot [20].

Kerr et al. [32] captured motion data using a tracking system with reflective markers and infrared cameras. They found differences in the inversion-eversion of the hindfoot and abduction–adduction of the forefoot between symptomatic and asymptomatic flat feet. Also, Buldt et al. [27] analyzed kinematic data captured from a camera-based motion capture system using optical markers, and found that during initial contact and mid-stance the cavus foot exhibited less motion in the sagittal and transverse planes; also, lower midfoot range of motion during the pre-swing of planus foot. Kruger et al. [28] also analyzed the kinematic characteristics of foot and ankle among normal, planus, and cavus feet. For that, the differences in the tibial angle, hindfoot angle, and forefoot angle were observed among the three foot types throughout the gait cycle. Differences were also found in the coronal forefoot angular velocity.

As to the automatic classification of the foot types based on plantar sensing, some progress has already been made through stationary devices. Barton et al. [24] classified foot types into normal foot, cavus foot, and hallux valgus using the maximum pressure during the stance phase. Xu et al. [25] extracted from plantar pressure four foot-arch indexes as features: Staheli index, Chippaux-Smirak index, arch index, and modified arch index. They used a classifier combining fuzzy logic and neural network to classify cavus foot and planus foot. Ramirez-Bautista et al. [48] divided the plantar pressure area into fourteen sub-areas, including five toes, five metatarsal heads, lateral and medial midfoot, and lateral and medial heel. Cavus foot and planus foot were classified by the use of fuzzy cognitive maps with a genetic algorithm for weight learning. For the classification of the normal foot and flexible planus foot based on the ground reaction force, Bertani et al. [9] used a heuristic optimization technique named Discard-Insert-Exchange to extract the most discriminative features automatically. In this method, three linear discriminative functions (LDEs) were used, where each function maps one of the GRF components in the form of a one-dimensional feature vector. A fourth LDF was used to obtain the final foot type classification result. Böhm et al. [11] used principal component analysis to extract the three independent eigenvectors from the kinematic data of flexible flatfoot. Then, the K-means algorithm was applied to cluster transformed data into two types of flexible flatfoot. In this process, the inversion data during the push-off phase were the most discriminant. Table 1 contains a list of the main works dedicated to foot type classification using gait analysis devices.

So far, there was no study to classify foot types using inertial sensing. However, some authors studied the locomotion characteristics of each foot type, Grech et al. [26] found that there was a significant difference in the acceleration at heal strike between cavus foot and normal foot, as well as between cavus foot and planus foot. In another study [31], no difference was found in the acceleration between the normal foot and planus foot. Also, in a comparison between cavus foot and planus foot difference was observed in forefoot adduction excursion and forefoot abduction velocity [30].

The above studies of motion patterns of each foot type confirm that foot types can be differentiated based on kinematic and kinetic characteristics. We thus hypothesized that obtaining those two kinds of information would allow for foot type screening. Hence, in this study, we suggest a proof-of-concept of a wearable system with integrated inertial and force sensors that can provide kinematic and kinetic information of foot motion, respectively. In previous studies, one-dimensional convolutional neural network (1D-CNN) has been successfully applied for processing motion sen-

Table 1
The devices and methods related to foot type classification.

Authors (Ref.)	Platform	Foot types	Samples # (training#, testing#)	Models	Result
Barton et al [24]	plantar pressure platform (EMED F)	Normal, cavus, hallux valgus	(28,13) (10,8)	neural network	92% 100%
Xu et al [25]	plantar pressure platform	cavus, planus	(300,200)	adaptive neuro-fuzzy inference system	95%
Bertani et al [9]	force plate (Kistler)	Normal, planus	112(leave-One-out test)	LDF-LC	84.8%
Böhm et al [11]	Motion capture system (Vicon Nexus)	Two types of flexible flatfeet	255	k-means	effective cluster
Ramirez-Bautista et al [48]	plantar pressure platforms (FreeMed)	Cavus, planus	151	GA-FCM	91%

sor time-series, in, e.g., golf swing classification [33], automatic detection of freezing gait of Parkinson disease [34] and real-time activity classification [35]. CNNs outperform conventional machine learning methods based on handcrafted features thanks to their ability to automatically extract features from the low to the high level of representation. Based on this evidence, we considered combining the wearable gait analysis system with a 1D CNN for the extraction of discriminative features. The suggested concept could eventually reflect the functional differences among the three types of foot. In practice, such systems could allow for real-time monitoring of foot status and early warning of foot deformities. To the best of our knowledge, the proposed concept is the first one for foot type classification based on a wearable system.

3. Experimental platform and data acquisition

3.1. Experimental platform

For the present study, we developed a full data acquisition framework, including a custom sensor insole. Fig. 1 illustrates the prototype of the insole and its main components.

The device incorporates nine force sensors of type FlexiForce A301 (Tekscan, Inc., USA) and an inertial sensor of type BMI160 (Bosch Sensortec GmbH). Force sensors were attached to a thin and flexible printed circuit board and located under the main weight-bearing areas of the foot, namely the hallux, five metatarsal heads, lateral midfoot, the lateral heel and medial heel. The inertial sensor contains a three-axis accelerometer and gyroscope. All sensor signals were sampled at 100 Hz, a rate acceptable when the locomotion type is walking at normal speed. The electronic control board, also holding the inertial sensor, was attached to the top of the shoe over the forefoot area. Force sensors allowed capturing kinetic information; inertial sensor provided kinematic information. The combination of the two modalities was expected to offer the highest accuracy of foot type classification. Sensor data were transferred wirelessly using Bluetooth technology to a custom receiver connected to a personal computer. Detailed information about the developed insole can be found in [36,37].

3.2. Data acquisition

The data collection procedure was conducted in accordance with the Declaration of Helsinki. Each subject was informed about the experimental procedure, and his/her agreement to participate in the experiment was obtained. A total of 80 subjects were recruited for the experiment. Only data of the left feet were processed in this study. Among all subjects, there were 44 subjects with normal feet, 16 with planus feet, and 20 with cavus feet. The type of each foot was determined and labeled by a podiatrist. Subjects' demographics data are listed in Table 2. Subjects with pain or injury in a foot, ankle, or knee, or who underwent surgery in these areas within the last six months before the data collection, were not recruited. Before the experiment, each subject was informed about the experimental procedure and asked to fill out a questionnaire about age, gender, height, weight, and health status related to the locomotor function. The latter required reporting of pain in the heel, mid-foot, forefoot or hallux, or problems in the back, knee, or hip, as well as a history of falls. For each foot, photos

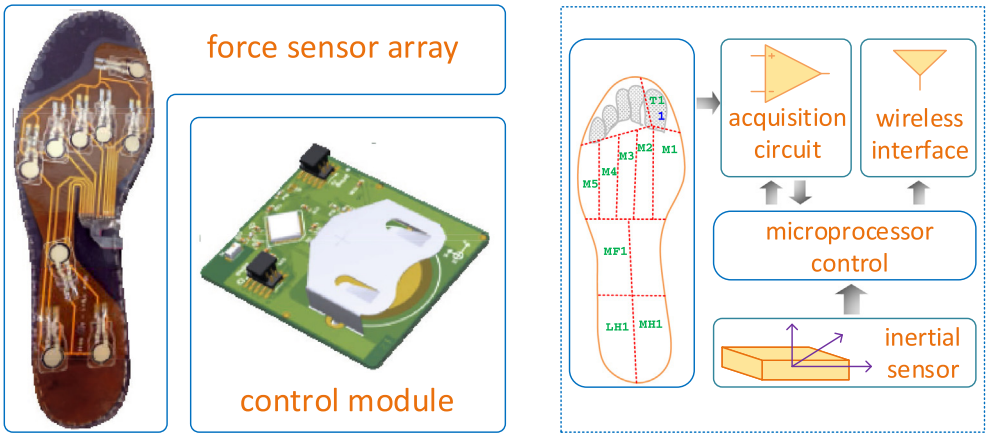

Fig. 1. The custom insole (a) implemented prototype (b) components.

Table 2
Demographic characteristics of the subjects.

Foot type	Gender (male/female)	Age (years old ± SD)	Height (cm ± SD)	Weight (kg ± SD)	Foot size (cm ± SD)
Normal (44)	31/13	21 ± 1.20	169.1 ± 8.3	61.7 ± 10.3	25.1 ± 1.3
Cavus foot (20)	15/5	21 ± 0.78	169.9 ± 5.9	61.0 ± 9.2	24.9 ± 1.1
Planus foot (16)	10/6	21 ± 0.78	168.7 ± 8.6	63.9 ± 10.5	25.1 ± 1.1
Total (80)	56/24	21 ± 1.19	169.2 ± 7.8	60.6 ± 10.1	25.0 ± 1.2

SD: standard deviation.

were taken of the medial longitudinal arch to examine the arch, and of the heel and tibia to examine the foot alignment during static standing. Each subject wore shoes with inserted sensor soles of an appropriate size. Data were acquired while each subject walked straight over a 7-meter walkway completing in this way seven or eight steps until arriving at the end of the walkway. Each trial covered the phases of gait initiation, gait stabilization, and gait termination. We hypothesized that collected data contain discriminative information for foot type classification. During the test, sudden changes in the gait were not allowed. Each subject performed approximately twenty trials. The data of some trials were considered invalid due to operator or subject mistakes. After discarding invalid trials, the data of 1488 trials were deemed valid. These included 827 records of normal feet, 343 of cavus feet, and 318 planus feet records. The experimental configuration is illustrated in Fig. 2. The waveforms of a valid representative trial are shown in Fig. 3.

4. Data analysis

4.1. 1D CNNxxx

CNN is a feed-forward neural network, inspired by the physiological structure and signal processes of the human visual cortex. 1D-CNN, 2D-CNN, and 3D-CNN are used to process 1D time series, 2D images, and image series, respectively. Four properties allow the benefits of the CNNs: the local connection, shared weights, pooling, and the use of multiple layers [38]. The typical structure of a CNN involves stacked convolutional layers, a pooling layer, and fully connected layers. Each convolutional layer represents a feature abstraction in space and/or time domain of the input data or the previous feature maps. The stacked convolutional layers lead to progressively extracted feature maps from the low-level abstraction to the high-level ones. Each pooling layer downsamples the features from the preceding maps without loss of information and, thus, reduces the dimension of the preceding map. Max pooling is generally used [38]. The activation function performs the non-linear mapping from the output of the previous neuron of the convolutional layer; this allows the network to learn a complex model [39]. Non-saturated activation functions, e.g., rectified linear unit (ReLU), which solve exploding or vanishing gradient, and speed up convergence, are widely used in deep learning [40]. To determine the appropriative activation function, several saturated activation functions, including ReLU, Leaky ReLU (LReLU), parametric ReLU (PReLU), randomized ReLU (RReLU), respectively, were explored in this study.

In the present study, to address the problem of the covariate shift, batch normalization was used in the 1D CNN architecture. The normalization accelerates the speed of network training and relieves the need to take care of the parameter initialization [41].

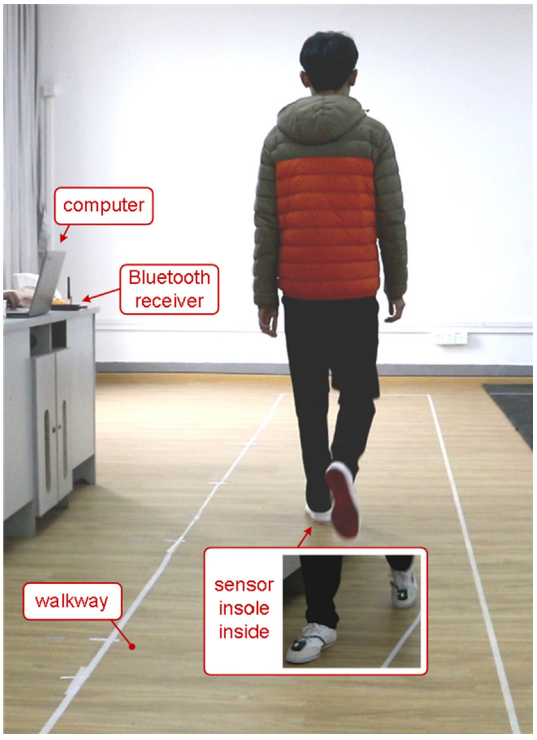

Fig. 2. Experimental configuration.

4.2. The proposed architecture

The basic processing model (BPM) that defines the 1D CNN architecture applied in this study is presented in Fig. 4 (a), and we applied it for all variants of input data. Data were first normalized with Z-scores and then fed to the corresponding BPM. Each module consisted of two convolutional layers and one max pool layer; each layer was followed by batch normalization and activation. The architecture of the 1D-CNN that fused all three modalities is shown in Fig. 4(b). Four modules were stacked during the stage of feature learning. Then the learned features from the three pipelines were concatenated and passed to a network consisting of a flatten layer, two fully connected layers, and one softmax layer with softmax activation. For every single type of data, there was no concatenating step for feature fusion.

We aimed to investigate which individual type of data and which fusion scheme would serve foot type classification better. For that purpose, we trained an individual model using acceleration, angular velocity, and force data, respectively. Then, we designed four feature fusion schemes: (1) acceleration and angular velocity, (2) acceleration and force (3) angular velocity and force, and (4) accelerometer, angular velocity, and force.

To find an appropriate pool size, we tested the sizes from 1×3 to 1×8. We also explored convolutional kernel sizes from 1×3 to 1×7, tested several activation functions, and batch sizes from 16 to 64 with an interval of 8. Because of the restricted computing power, we were not able to find a global optimization of the parameters and, as a workaround, adopted a greedy search. First, we adjusted the convolutional kernel size; then, based on the optimized kernel size, we adjusted the pool size. We adopted a similar strategy to adjust the activation function and the batch size.

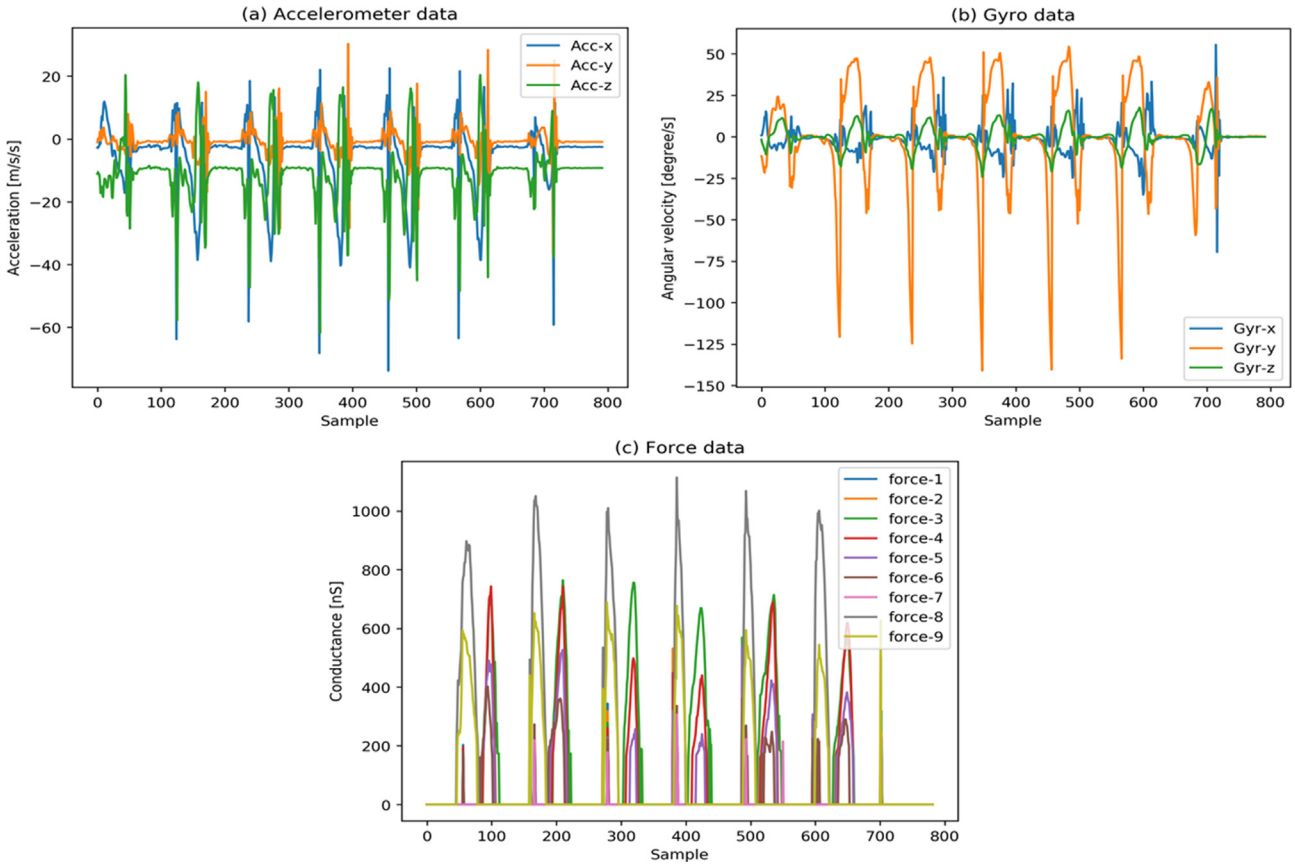

Fig. 3. Waveforms of a valid representative recording.

4.3. Model training

We trained each of the models for 100 epochs. Categorical Cross-Entropy served as a loss function, and Adadelta optimizer was applied to update the model parameters. A specific characteristic of the Adadelta optimizer is that the learning rate decreases monotonically with the progression of learning [42]. The accuracy and loss of training and testing were saved for each epoch, and the model of the last epoch was saved for the prediction.

5-fold cross-validation: To evaluate the generalization capability of the 1D-CNNs and the conventional models for foot type classification, we performed a stratified 5-fold cross-validation, in which each fold kept the same proportion of samples for each given category. For that, all samples were partitioned into five subsets. One subset of data was used to test the trained model; from the rest subsets, 20% were used for validation and 80% for training. This process was repeated five times until using each subset as a test set. The performance of each classifier was evaluated based on the resulting confusion matrix. For each confusion matrix, each row represents the instances of the actual class, while each column represents the ones of the predicted class. Four average metrics: recall, precision, f-measure, and accuracy, obtained from the matrix, were also used for evaluating the performance of the models. The 5-fold cross-validation was performed over each of the input data variants.

4.4. Technical specification

The algorithm was implemented using Python 3.6 and Keras 2.2.4 with TensorFlow-GPU 1.12.0. It was executed on a computer provided with Intel® Core (TM) i7-7800X CPU, 32 GB RAM, and Windows 10. Additionally, a GPU NVIDIA TITAN Xp, with 12 GB GDDR5X and 3840 cores was used to accelerate the processing.

4.5. Comparison with conventional machine learning methods

A third-order Butterworth low pass filter with a cutoff frequency of 16 Hz was applied to each of the three types of data [14]. The handcrafted features obtained from insole data were the maximum, minimum, mean, range, zero-crossing rate, root-mean-square value, variance, standard variance, skewness, and kurtosis. For the comparison, in the role of conventional methods, Random forest, support vector machine (SVM), and decision tree were used to classify the foot types based on the handcrafted features.

Random forest is an ensemble learning method suitable to process foot motion data [44]. It consists of a collection of trees, each of which builds on randomly sampled data that have the same statistical distribution as ones of all other trees in the forest. For classification in the forest tree, voting is typically used to determine the class labels. We used a grid search to determine optimal values of the number of trees, maximum depth, and the number of features to split each node [47].

The SVM is a supervised machine learning technique. It is based on the statistical learning theory of Vapnik–Chervonenkis dimension and structural risk minimization. An SVM constructs the hyperplanes with maximum margin to separate the data into different classes [46]. A kernel function could be introduced to project the data into a higher dimension, which allows making the data linearly separable. Among kernel functions, SVM with radial basis function showed the best accuracy in this study. The parameter of the decision function shape was selected as "one against the rest". The parameters C and γ of the SVM were explored using a

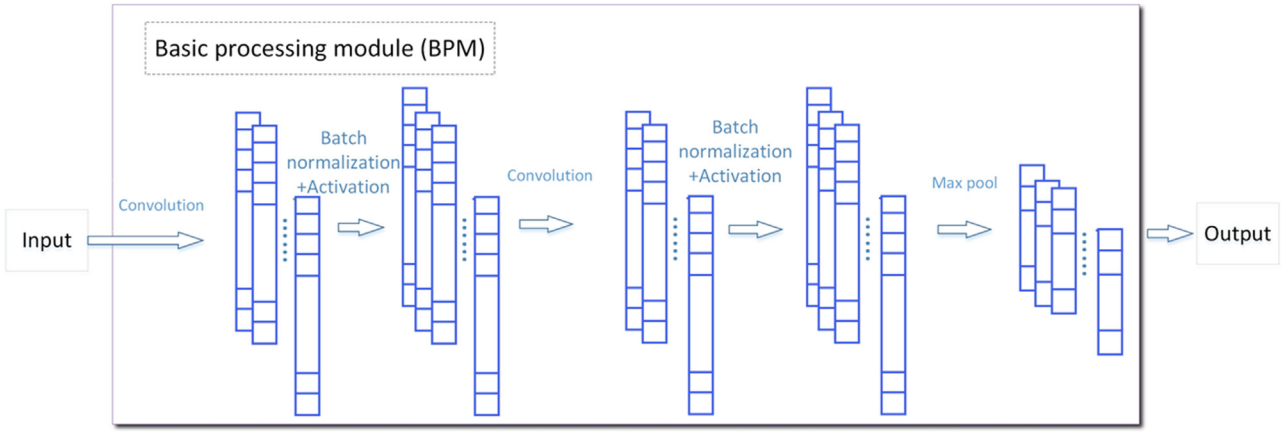

(a)

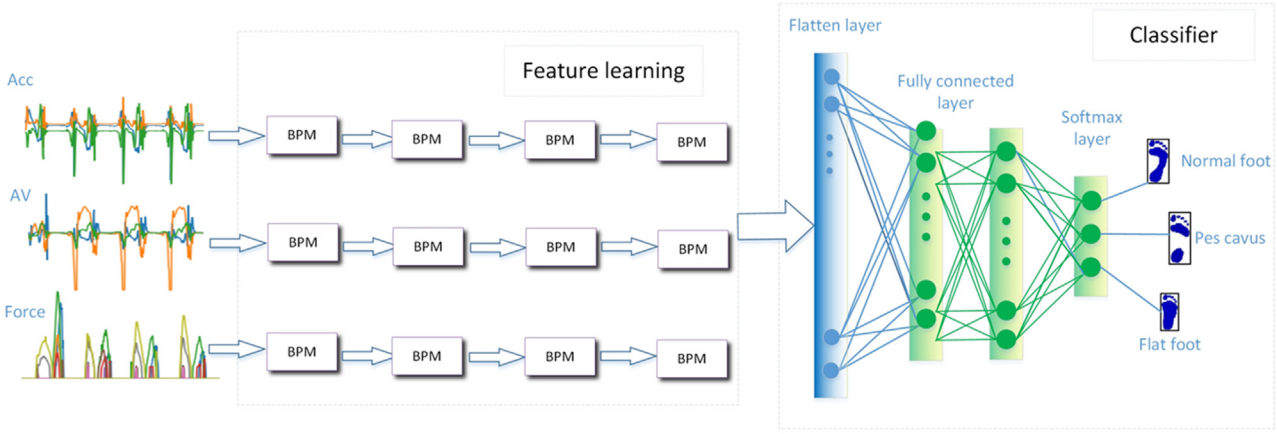

(b)

Fig. 4. The architecture of the 1D-CNN with a fusion of features from the three types of data. (a) The basic feature extraction module (BPM); it consists of two stacked convolutional layers and one pooling layer. Each convolutional layer was followed by batch normalization and function activation. (b) A representative fusion model. After the last pooling layer, the features of the separate maps were concatenated; they were then passed to a network consisting of a flatten layer, two fully connected layers, and a softmax layer. We used four modules similar to the representative one, to extract features of each variant of input data, respectively.

grid search. PCA was used to project the handcrafted features to improve the performance of the SVM.

A decision tree is a tree-like classifier based on data partitioning [45]. Each internal node splits the data into subsets according to the features. Each edge represents the outcome of the partitioning. Each leaf node represents a class label. The decision tree is an algorithm that does not require domain knowledge or parameter setting. It can handle different types of data without transformation, and can also process multidimensional data. In this study, a grid search was used to find the appropriate values for the maximum depth and the number of features. The ranges of the hyperparameters for the three algorithms are provided in Table 3. All the conventional machine learning algorithms used in the study are a part of the Python library Scikit-learn 0.19.1.

5. Results

5.1. Parameter optimization

For finding the optimal parameters of the 1D CNNs, grid search was performed, which started with defaults as follows: activation function PReLU; kernel size, and pool size of 1×3; a batch size of 32. We first searched the optimal kernel size with default settings; then, using the optimal kernel size and default batch size and activation function, we searched for the optimal pool size. The rest parameters were optimized using similar steps. The optimized parameters for all seven 1D CNN models that cover the three types of individual data and the modality combinations are shown in Fig. 5(a)–(d). The optimized parameters in the final models for each type of data and the combination of the data are listed in Table 4.

After the 5-fold cross-validation, the model built on acceleration data had the following optimal parameters: convolutional kernel size of 1×5, pool size of 1×7, ELU activation function, and a batch size of 32. The best average accuracy of the model on the test set reached 95.16%. The accuracy and loss on the training set and validation set for acceleration data and optimized kernel size are shown in Fig. 6(a)–(e).

5.2. Recognition of foot types

Fig. 7a–g present the confusion matrices of each five-fold cross-validation for the individual and combined modality models. With

Table 3
Ranges of the hyper-parameters.

Classifier	Parameters	Range
Random Forest	Number of trees	20–128
	Maximum depth	Acc, AV: [None, 10, 20, 30, 40, 50, 60] Acc + AV: [None, 10, 20, 30, 40, 50, 60, 80, 100, 120] Force:[None, 10, 20, 30, 40, 50, 60, 80, 100, 120, 140, 160, 180] Acc + force, AV + force: [None, 10, 20, 30, 40, 50, 60, 80, 100, 120, 140, 160, 180, 200, 220, 240] Acc + AV + force: [None, 10, 20, 30, 40, 50, 60, 80, 100, 120, 140, 160, 180, 200, 220, 240, 260, 280, 300]
	Number of features	[None, 'sqrt']
Decision tree	Maximum depth	Acc, AV: [None, 10, 20, 30, 40, 50, 60] Acc + AV: [None, 10, 20, 30, 40, 50, 60, 80, 100, 120] Force:[None, 10, 20, 30, 40, 50, 60, 80, 100, 120, 140, 160, 180] Acc + force, gyr + force: [None, 10, 20, 30, 40, 50, 60, 80, 100, 120, 140, 160, 180, 200, 220, 240] Acc + AV + force: [None, 10, 20, 30, 40, 50, 60, 80, 100, 120, 140, 160, 180, 200, 220, 240, 260, 280, 300]
	Number of features	[None, 'sqrt']
SVM	C	[0.01, 0.1, 1, 10, 100]
	γ	[0.00001, 0.001, 0.01, 0.1, 1]

None: The search for the best split was performed using all features.
Sqrt: The search for the best split was performed using the square root of all features.

force data being an individual modality, only 16 samples were misclassified, which is lower than the other two individual modalities. The model misclassified 11 samples when using the combination of the acceleration (Acc) and force data, angular velocity (AV) and force data, and all types of data, respectively.

The metrics for evaluating the performance of individual data models and those constructed using different modality combinations are illustrated in Table 5. The metrics of the model obtained from force data were higher than those of the single-modality models obtained from acceleration and angular velocity, respectively. All average accuracies after the five-fold cross-validation were above 95%. The model using force achieved an average accuracy of 98.92%. As to the sensor combinations, acceleration and angular velocity determined the lowest average accuracy of 97.91%, which was lower than using force sensor data only. The other combinations led to almost identical average accuracy, but with different precision, recall, and F-measure. Angular velocity and force data allowed for better recognition of cavus foot with a recall of 0.992. The model using all types of data together determined a recall of 0.996 for the normal foot, which is better than

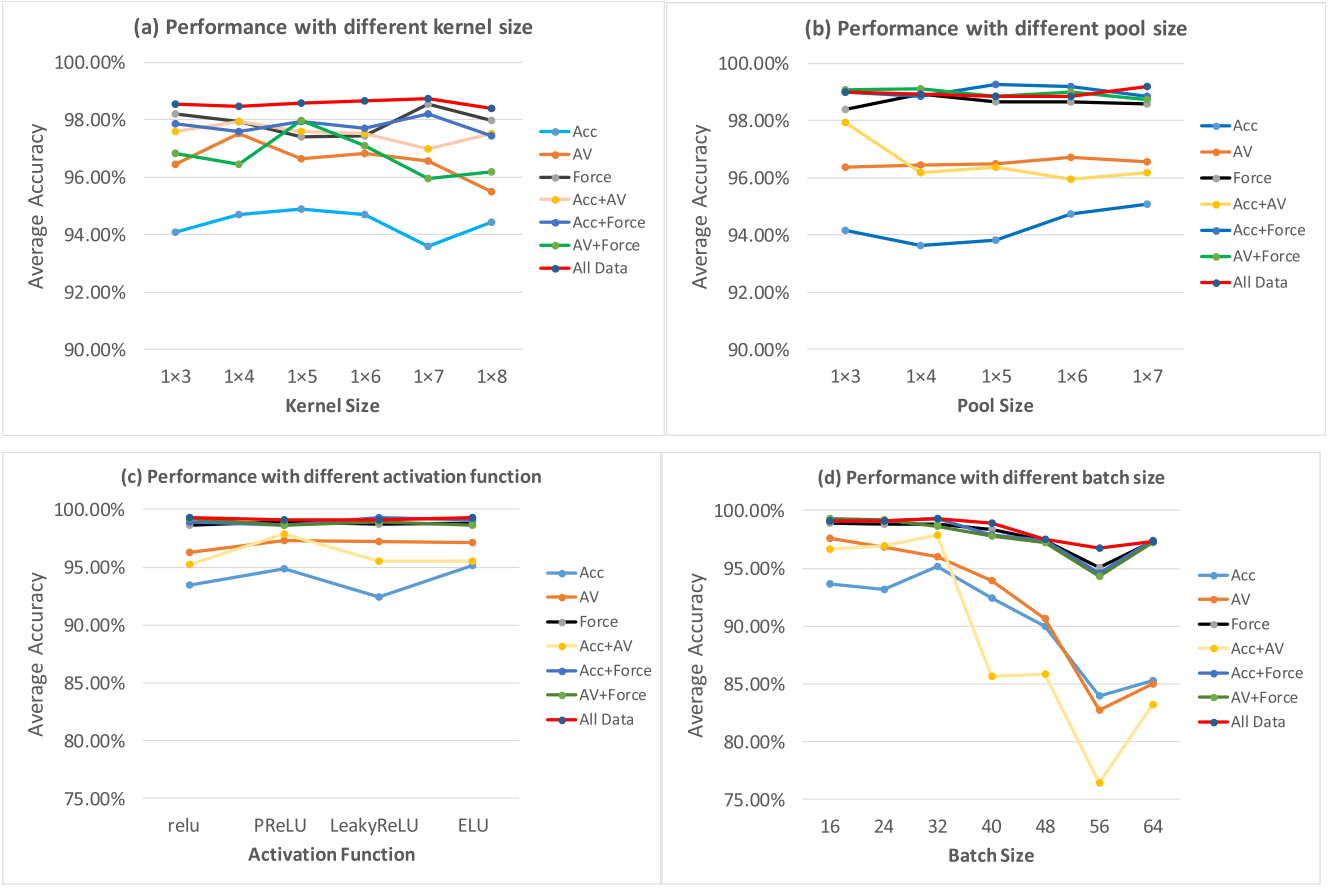

Fig. 5. Performance of 1D CNNs with optimal parameters. Average accuracies with different (a) kernel size (b) pool size (c) activation function and (d) batch size.

Table 4
Optimal parameters were used for the final models.

Data	Kernel size	Pool size	Activation function	Batch size
Acc	1 × 5	1 × 7	ELU	32
AV	1 × 4	1 × 3	PReLU	16
Force	1 × 7	1 × 4	PReLU	16
Acc + AV	1 × 4	1 × 3	PReLU	32
Acc + force	1 × 7	1 × 5	PReLU	32
AV + force	1 × 5	1 × 4	ReLU	16
All data	1 × 7	1 × 7	ReLU	32

when using combinations of two modalities. Among the classified samples, the best precision of 100% was achieved for cavus foot using acceleration and force data. For planus foot, the best precision was 0.992 using the combination of three modalities. For normal foot, the best precision of 0.994 was obtained using angular velocity and force data.

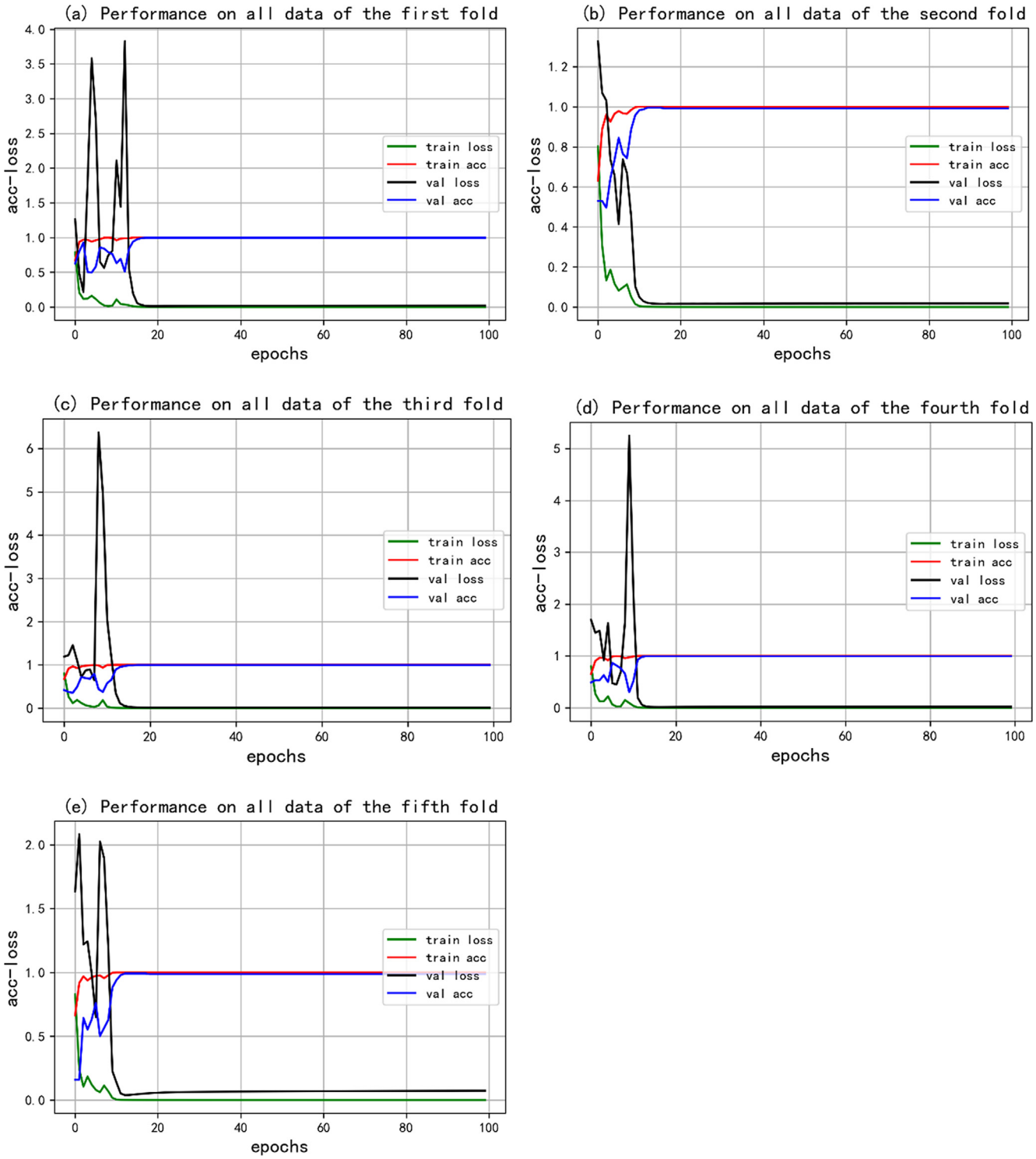

Fig. 6. Representative accuracy and loss of the model built on Acc data with optimal convolutional kernel size during the 100 epochs.

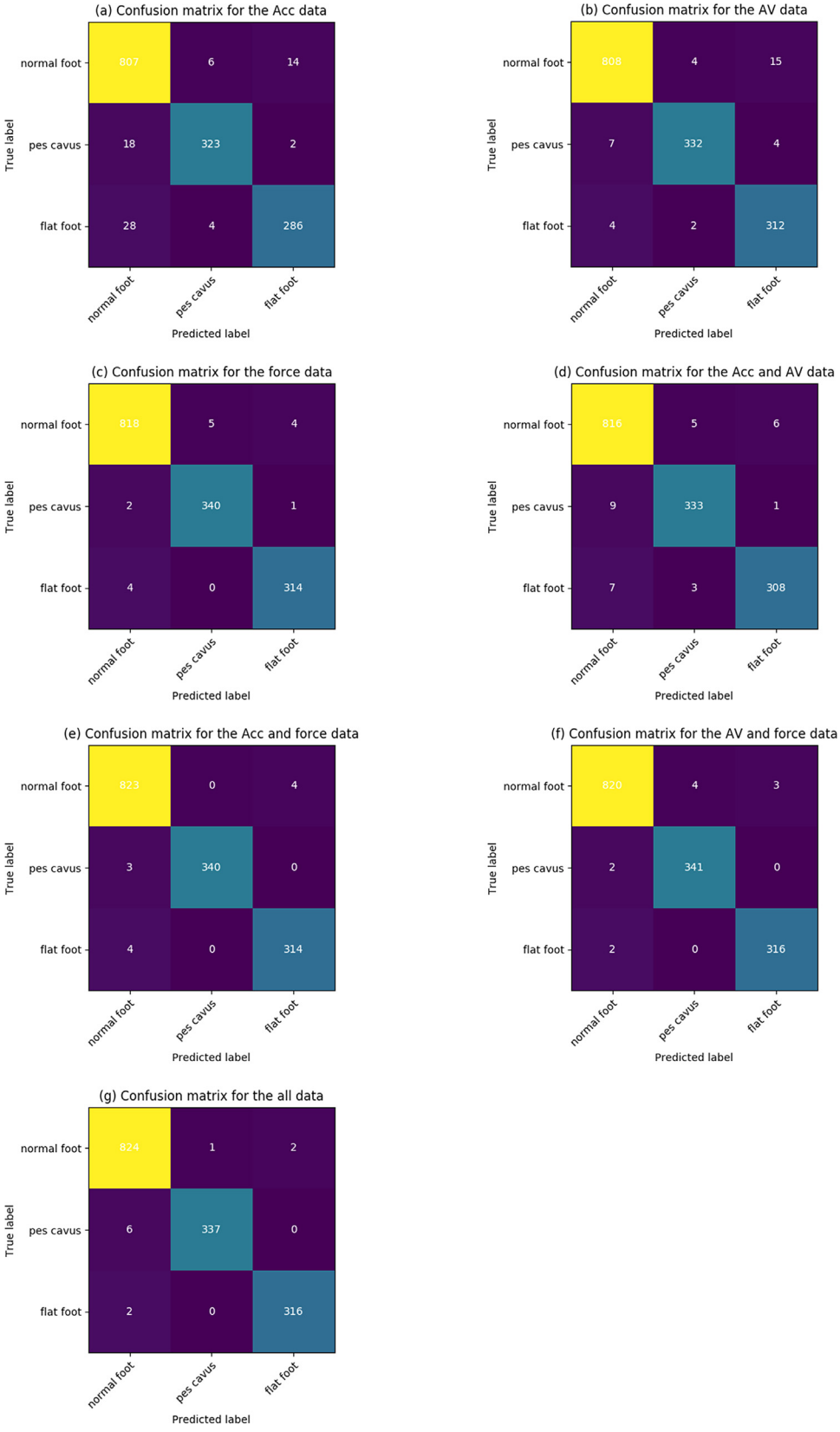

Fig. 7. Accumulative confusion matrix for each type of sensor data and their combination.

5.3. Comparison with conventional methods

To demonstrate the characteristics of the deep learning method, random forest, SVM with PCA, and decision tree were performed with handcraft features; the results are presented in Table 6. The average accuracies on all individual modalities and their combinations were above 93%, 95%, and 79% for the three methods, respectively. Among the three conventional methods and the 1D-CNNs,

Table 5
Average metrics for individual modalities and modality combinations.

Data	Foot type	Precision		Recall		F-measure		Accuracy	
		Mean	SD	Mean	SD	Mean	SD	Mean	SD
Acc	Normal foot	0.946	0.0185	0.976	0.012	0.962	0.0075	0.9516	0.0080
	Cavus foot	0.97	0.0179	0.942	0.0213	0.956	0.0162		
	Planus foot	0.95	0.0316	0.902	0.0264	0.922	0.0098		
AV	Normal foot	0.986	0.0049	0.976	0.0162	0.982	0.0098	0.9758	0.0147
	Cavus foot	0.982	0.0223	0.97	0.0329	0.974	0.0242		
	Planus foot	0.944	0.0361	0.98	0.0190	0.962	0.0286		
Force	Normal foot	0.992	0.0075	0.988	0.004	0.988	0.0074	0.9892	0.0065
	Cavus foot	0.988	0.0098	0.992	0.016	0.988	0.0098		
	Planus foot	0.982	0.0098	0.986	0.012	0.986	0.008		
Acc + AV	Normal foot	0.98	0.0167	0.984	0.0136	0.984	0.0049	0.9791	0.0112
	Cavus foot	0.978	0.016	0.972	0.0214	0.974	0.0150		
	Planus foot	0.978	0.0223	0.966	0.0377	0.972	0.0204		
Acc + force	Normal foot	0.992	0.0075	0.994	0.0049	0.992	0.004	0.99262	0.0044
	Cavus foot	1	0	0.992	0.0117	0.996	0.0049		
	Planus foot	0.986	0.012	0.986	0.012	0.986	0.008		
AV + force	Normal foot	0.994	0.008	0.99	0.0063	0.994	0.0049	0.99262	0.0053
	Cavus foot	0.99	0.0155	0.994	0.012	0.992	0.0075		
	Planus foot	0.988	0.0098	0.992	0.0098	0.99	0.0063		
Acc + AV + force	Normal foot	0.992	0.0075	0.996	0.0049	0.992	0.004	0.99261	0.0032
	Cavus foot	0.998	0.004	0.984	0.0162	0.99	0.0063		
	Planus foot	0.992	0.0098	0.992	0.0098	0.992	0.004		

SD: standard deviation.

Table 6
The average accuracy of each classification method.

Data	Random forest		PCA + SVM		Decision tree		Proposed method	
	Mean	SD	Mean	SD	Mean	SD	Mean	SD
Acc	0.9475	0.0089	**0.9771**	0.0081	0.7910	0.0062	0.9516	0.0080
AV	0.9369	0.0103	0.9583	0.0033	0.7957	0.0207	**0.9758**	0.0147
force	0.9845	0.0063	0.9832	0.0061	0.8818	0.0172	**0.9892**	0.0065
Acc + AV	0.9718	0.0061	0.9885	0.0078	0.8193	0.0298	**0.9791**	0.0112
Acc + force	0.9913	0.0055	0.9858	0.0039	0.8972	0.0128	**0.99262**	0.0044
AV + force	0.99260	0.0033	0.9886	0.0027	0.8757	0.0163	**0.99262**	0.0053
Acc + AV + force	**0.9940**	0.0039	0.9913	0.0017	0.8751	0.0193	0.99261	0.0032

SD: standard deviation.

decision tree had the lowest performance when individual modalities, as well as their combinations, were used. SVM with PCA showed the best performance among four methods with an average accuracy of 0.977 on Acc data, and 0.9885 on the combination of Acc and force data, respectively. Random forest outperformed other classifies with an average accuracy of 99.40 on all types of data.

6. Discussion

In this study, we proposed a set of 1D-CNNs to effectively classify three types of feet using acceleration, angular velocity, and force data. Each type of data allows reaching an average accuracy of over 95%. This result proves that the CNN model can extract the most discriminative features from our insole data. However, the performances of models constructed on different combinations of sensor data were different. When used individually, force data allowed achieving the best average accuracy. This result implies that the forces acquired from the main anatomical positions of the foot can serve as a reliable indicator of the differences in the gait patterns among the three explored foot types. So far, foot type classification was always based on analysis of plantar pressure distribution measured using force sensor arrays. Such an approach requires large volumes of force sensor data to be collected, processed and stored. Also, it is associated with a high cost of the data collecting system, especially when compared with a portable device with just a few force sensors. These conclusions are supported by Hsu et al. [43], where an ink footprint was compared with low-spatial-resolution force sensor data, and a high correlation was found for the medial arch in static testing and the lateral arch in dynamic testing. However, the authors only found the statistical correlation, while no classifier was constructed.

As for the classification of foot types based on the acceleration and angular velocity data, to our best knowledge, no study explored this topic. In several studies [26,30,31], only statistical difference was explored. However, those differences indicate that the locomotion patterns of the foot types are different, and it is possible to classify the foot types based on inertial data. The present study confirms this assumption. Among classifiers constructed in this study, the models that combined features of multiple types of data achieved better results. During a gait cycle, the foot performs dorsiflexion/plantar flexion, eversion/inversion, and abduction/adduction. The acceleration and angular velocities reflect the kinematic characteristics of these motions, while the force sensor indicates the vertical ground reaction force under the main plantar areas. Each modality represents different motion characteristics of the foot; thus, the fusion strategy allows obtaining the highest number of discriminative features for best classification performance.

For automatic classification of foot types, Xu et al. [25] used adaptive neuro-fuzzy inference system as a classifier; they extracted four kinds of arch indexes from plantar pressure and used these as features; the obtained model reached an accuracy of 95% for classification of planus and cavus feet. Also, Ramirez-

Bautista et al. [48] divided the area of the plantar pressure into fourteen sub-areas. To classify planus and cavus feet, they applied Fuzzy Cognitive Maps with a genetic algorithm for weight learning and achieved an accuracy of 91%. In this study, we classify foot types into normal, cavus, and planus foot based on data collected through our insole and classified using a 1D CNN. Through our approach, we reached an accuracy of more than 99.26%. That result was possible thanks to the integration of both inertial and force sensors, which allows obtaining richer motion information in contrast with systems using solely plantar pressure. Besides, 1D CNN offers the advantage of extracting discriminative features automatically, in contrast to using hand-crafted features that might be suboptimal. A possible drawback of our solution in comparison with traditional classification methods is that the classification algorithm requires more computational power, especially in the training phase.

In the study, not all individual modality deep learning models outperformed the conventional methods. One of the possible reasons is that features that were automatically extracted by the 1D-CNNs were different from those used with the conventional methods; the second possible reason lies in the differences in the optimization methods. Because of the limitation of the computing power of the station used to construct the deep learning models, we adopted a greedy search approach that cannot guarantee an optimal global result. For the three conventional methods, we used a grid search for the essential parameters, and it was possibly better than the greedy search. The third possible reason is that when used deep learning methods, higher volumes of data are needed since these methods rely on learning a high number of parameters, typically exceeding one million. Another limitation is that the age group of the subjects was restricted as all of them were university students. In our future studies, more subjects covering all age groups will be explored to allow for a better generalization ability of the deep models.

7. Conclusions and future work

Collaborative advances in sensing and textiles pave the way of smart footwear. One essential use of such technologies would be the automatic early detection of foot abnormalities. It has the potential to compensate for the lack of enough podiatrist resources and difficulties to establish mass foot screening. So far, however, little has been done to validate the feasibility of distinguishing foot types based on a wearable device. To make a step towards filling this gap, in this study, we used a custom, fully-featured framework to collect and analyze walking data from normal, cavus, and planus feet. It involved sensor insoles incorporating inertial and force sensors for the signal collection and a set of 1D CNN models. For comparative evaluation of the 1D CNN model performance, three conventional machine learning methods with handcrafted features were also applied to classify foot types. Force data allowed for the best performance compared with individually used acceleration and angular velocity data. In most cases, combinations of force data with one of the other two modalities allowed for a better result than that of a single modality.

With the present study, we validate the feasibility of automatic foot types classification through the use of a wearable system for gait analysis. Because of factors including the up-until-recently-limited availability of the required technologies to build unobtrusive and practical sensor-enabled footwear, applications of wearable system-based gait analysis are yet to make their way in practice. Existing commercial sensor-enabled footwear products mainly address diabetic foot monitoring, and fitness uses. In contrast, the concept we suggest could allow for real-time monitoring of the foot function and early warning of foot deformities. Such solutions are very needed as the in-lab mass screening is challenging to implement; on the other side, the target group of the proposed system is individuals with limited access to regular podiatrist care who need foot monitoring or those who are unaware of possible issues with their foot function. The first group is usually represented by the elderly or patients who had surgery or are under rehabilitation and need regular foot function monitoring; also, the users of foot orthoses. On the other side, youngsters are often unaware of possible issues with their foot function and the necessary corrective measures. In that case, an early warning would allow avoiding the long-term complications of untreated foot deformity. Long-term observations of foot type could also contribute to proper footwear selection.

As to the possible disadvantages of the proposed concept, these are mostly related to the technical possibilities to build an unobtrusive, convenient device with high user acceptance. We believe that most of the technical challenges are solvable with the current level of technologies, e.g., force sensors and matrices can be customized relatively easily, and new force sensor materials are taking place, such as graphene. Also, in this study, we propose a proof-of-concept. However, for a real-world application, different technical details and the system components are to be determined. For instance, our current classification method is based on a 1D CNN that may naturally be computationally heavy. In our future studies, we need to test if the classification can be executed on a smartphone and whether models can be optimized for use in edge systems. If the processing is not possible locally, data need to be transmitted to a cloud that will return the result of processing. Then, in case of limited connectivity to servers, problems with the real-time display of foot status may also arise.

In the near future, we are going to implement improvements in both hardware and algorithmic aspects. At the system level, we are going to increase the number of force sensors to obtain a more detailed picture of dynamic plantar pressure patterns. With increasing the number of sensors in the new design, the matter of data volume optimization will become critical, which we will address through the methods of compressive sensing. For the research of foot types classification, we consider involving 3D force and moments sensing such as Xsens ForceShoe; it will allow measuring the foot and ankle motion in medial–lateral, fore-and-aft, and vertical directions, thus contributing to obtaining a more discriminative motion pattern. In terms of data processing and algorithms, we will continue collecting and annotating foot type data; with increasing the size of the training datasets, the generalization ability of trained models is expected to improve.

One of the open questions in both theoretical and practical aspects of artificial intelligence methods is that the complex nonlinear models are viewed as black-box classifiers. Hence, approaches are required to allow explaining the decisions of the classifier and the contribution of each input variable to the classification output. In a theoretical aspect, such techniques will allow for a more in-depth understanding of factors determining the classifier decisions; from a practical perspective, knowing which input variables are most significant will make it possible to optimize the whole pipeline from data collection at the sensor node to obtaining the high-level classification result. In our future work, we will analyze factors determining classifier decision and the contribution of input variables, applying techniques such as the Layer-Wise Relevance Propagation [49].

CRediT authorship contribution statement

Zhanyong Mei: Investigation, Data curation, Software, Writing - original draft. **Kamen Ivanov:** Data curation, Software, Writing - review & editing. **Guoru Zhao:** Validation, Visualization. **Yua-**

nyuan Wu: Visualization, Writing - review & editing. **Mingzhe Liu:** Conceptualization, Writing - review & editing. **Lei Wang:** Supervision.

Declaration of Competing Interest

The authors declare that they have no known competing financial interests or personal relationships that could have appeared to influence the work reported in this paper.

Acknowledgment

This project was supported in parts by the NSFC under grant no. U19A2086 and Grant no. 61701049, Key Project 2017GZ0304 of the Science and Technology Department of Sichuan province and the young and middle-aged backbone teachers' program of Chengdu University of Technology.

References

[1] N. Shibuya, L.J. Ciliberti, D.C. Jupiter, V. VanBuren, J.L. Fontaine, Characteristics of Adult Flatfoot in the United States, J. Foot Ankle Surg. 49 (4) (2010) 363–368.
[2] E. Sadeghi-Demneh, J.M.A. Melvin, K. Mickle, Prevalence of pathological flatfoot in school-age children, Foot 37 (2018) 38–44.
[3] V. Sachithanandam, B. Joseph, The influence of footwear on the prevalence of flat foot. A survey of 1846 skeletally mature persons, J. Bone Joint Surg. Br. 77 (2) (1995) 254–257.
[4] B.S. Neal, I.B. Griffiths, G.J. Dowling, G.S. Murley, S.E. Munteanu, M.M.F. Smith, N.J. Collins, C.J. Barton, Foot posture as a risk factor for lower limb overuse injury: a systematic review and meta-analysis, J. Foot Ankle Res. 7 (55) (2014) 1–13.
[5] P. Wicart, Cavus foot, from neonates to adolescents, Orthopaed. Traumatol. Surg. Res. 98 (7) (2012) 813–828.
[6] A.S. Eleswarapu, B. Yamini, R.J. Bielski, Evaluating the Cavus Foot, Pediatr. Ann. 45 (6) (2016) e218.
[7] A. Manoli, B. Graham, Clinical and new aspects of the subtle cavus foot: A review of an additional twelve year experience, Fuß & Sprunggelenk 16 (1) (2018) 3–29.
[8] M. Razeghi, M.E. Batt, Foot type classification: a critical review of current methods, Gait Post. 15 (3) (2002) 282–291.
[9] A. Bertani, A. Cappello, M.G. Benedetti, L. Simoncini, F. Catani, Flat foot functional evaluation using pattern recognition of ground reaction data, Clin. Biomech. 14 (7) (1999) 484–493.
[10] A.D. Cock, T. Willems, E. Witvrouw, J. Vanrenterghem, D.D. Clercq, A functional foot type classification with cluster analysis based on plantar pressure distribution during jogging, Gait Post. 23 (3) (2006) 339–347.
[11] H. Böhm, C. Oestreich, R. Rethwilm, P. Federolf, L. Döderlein, A. Fujak, C.U. Dussa, Cluster analysis to identify foot motion patterns in children with flexible flatfeet using gait analysis—A statistical approach to detect decompensated pathology?, Gait Post. 71 (2019) 151–156.
[12] A. Jafarnezhadgero, S.H. Mousavi, M. Madadi-Shadd, J.M. Hijmans, Quantifying lower limb inter-joint coordination and coordination variability after four-month wearing arch support foot orthoses in children with flexible flat feet, Hum. Mov. Sci. 70 (2020) 102593.
[13] K. Stanković, T. Huysmans, F. Danckaers, J. Sijbers, B. Booth, Subject-specific identification of three dimensional foot shape deviations using statistical shape analysis, Expert Syst. Appl. 151 (2020) 113372, https://doi.org/10.1016/j.eswa.2020.113372. https://linkinghub.elsevier.com/retrieve/pii/S0957417420301974.
[14] T.P. Fong, Y.Y. Chan, The Use of Wearable Inertial Motion Sensors in Human Lower Limb Biomechanics Studies: A Systematic Review, Sensors 10 (12) (2010) 11556–11565.
[15] C.A. Ronao, S.B. Cho, Human activity recognition with smartphone sensors using deep learning neural networks, Expert Syst. Appl. 59 (2016) 235–244.
[16] J. Hannink, T. Kautz, C.F. Pasluosta, K.G. Gasmann, J. Klucken, B.M. Eskofier, Sensor-based gait parameter extraction with deep convolutional neural networks, IEEE J. Biomed. Health. Inf. 21 (1) (2017) 85–93.
[17] J. Song, H.J. Hillstrom, M. Neary, K. Choe, W. Brechue, R.A. Zifchock, et al., Dynamic barefoot plantar pressure in gait and foot type biomechanics, J. Foot Ankle Res. 7 (1 Supplement) (2014) A77.
[18] S.S. Lee, S.T. Choi, S.-I.I. Choi, Classification of Gait Type Based on Deep Learning Using Various Sensors with Smart Insole, Sensors. 19 (8) (2019).
[19] A.K. Buldt, S. Forghany, K.B. Landorf, G.S. Murley, P. Levinger, H.B. Menz, Centre of pressure characteristics in normal, planus and cavus feet, J. Foot Ankle Res. 11 (3) (2018) 1–9.
[20] B. Chuckpaiwong, J.A. Nunley, N.A. Mall, R.M. Queen, The effect of foot type on in-shoe plantar pressure during walking and running, Gait Post. 28 (3) (2008) 405–411.
[21] T.C. Chao, B.C. Jiang, A comparison of Postural Stability during Upright Standing between Normal and Flatfooted Individuals Based on COP-Based Measures, Entropy 19 (2) (2017) 1–13.
[22] R. Tahmasebi, M.T. Karimi, B. Satvati, F. Fatoye, Evaluation of Standing Stability in Individuals With Flatfeet, Foot Ankle Spec. 8 (3) (2015) 168–174.
[23] W.R. Ledoux, H.J. Hillstrom, The distributed plantar vertical force of neutrally aligned and pes planus feet, Gait Post. 15 (1) (2002) 1–9.
[24] J.G. Barton, A. Lees, Development of a connectionist expert system to identify foot problems based on under-foot pressure patterns, Clin. Biomech. 10 (7) (1995) 385–391.
[25] S. Xu, X. Zhou, Y.N. Sun, A novel gait analysis system based on adaptive neuro-fuzzy inference system, Expert Syst. Appl. 37 (2) (2010) 1265–1269.
[26] C. Grech, C. Formosa, A. Gatt, Shock attenuation properties at heel strike: Implications for the clinical management of the cavus foot, J. Orthopaed. 13 (3) (2016) 148–151.
[27] A.K. Buldt, P. Levinger, G.S. Murley, H.B. Menz, C.J. Nester, K.B. Landor, Foot posture is associated with kinematics of the foot during gait: A comparison of normal, planus and cavus feet, Gait Post. 42 (1) (2015) 42–48.
[28] K.M. Kruger, A. Graf, A. Flanagan, B.D. McHenry, H. Altiok, P.A. Smith, G.F. Harris, J.J. Krzak, Segmental foot and ankle kinematic differences between rectus, planus, and cavus foot types, J. Biomech. 94 (2019) 180–186.
[29] A.K. Buldt, S. Forghany, K.B. Landorf, P. Levinger, G.S. Murley, H.B. Menz, Foot posture is associated with plantar pressure during gait: A comparison of normal, planus and cavus feet, Gait Post. 62 (2018) 235–240.
[30] A. Barnes, J. Wheat, C.E. Milner, Fore- and rearfoot kinematics in high- and low-arched individuals during running, Foot Ankle Int. 32 (7) (2011) 710–716.
[31] W.R. Ledoux, H.J. Hillstrom, Acceleration of the calcaneus at heel strike in neutrally aligned and pes planus feet, Clin. Biomech. 16 (7) (2001) 608–613.
[32] C.M. Kerr, A.B. Zavatsky, T. Theologis, J. Stebbins, Kinematic differences between neutral and flat feet with and without symptoms as measured by the Oxford foot model, Gait Post. 67 (2019) 213–218.
[33] L.B. Jiao, H. Wu, R.F. Bie, A. Umek, A. Kos, Multi-sensor Golf Swing Classification Using Deep CNN, Procedia Comput. Sci. 129 (2018) 59–65.
[34] J. Camps, A. Samà, M. Martín, D. Rodríguez-Martín, C. Pérez-López, J.M. Moreno Arostegui, J. Cabestany, A. Català, S. Alcaine, B. Mestre, A. Prats, M.C. Crespo-Maraver, T.J. Counihan, P. Browne, L.R. Quinlan, G. Laighin, D. Sweeney, H. Lewy, G. Vainstein, Alberto Costa, R. Annicchiarico, À. Bayés, A. Rodríguez-Molinero, Deep learning for freezing of gait detection in Parkinson's disease patients in their homes using a waist-worn inertial measurement unit, Knowl.-Based Syst. 139 (2018) 119–131, https://doi.org/10.1016/j.knosys.2017.10.017. https://linkinghub.elsevier.com/retrieve/pii/S0950705117304859.
[35] D. Ravi, C. Wong, B. Lo, G.Z. Yang, A deep learning approach to on-node sensor data analytics for mobile or wearable devices, IEEE J. Biomed. Health. Inf. 21 (1) (2017) 56–64.
[36] K. Ivanov, Z.Y. Mei, L. Lubich, N. Guo, X.L. Deng, Z.C. Zhao, O.M. Omisore, D. Ho, L. Wang, Design of a Sensor Insole for Gait Analysis, ICIRA 2019 (2019) 433–444.
[37] K. Ivanov, Z.Y. Mei, L. Lubich, L. Wang, Recognition of Pes Cavus Foot Using Smart Insole: A Pilot Study, ICIRA 2019 (2019) 654–662.
[38] Y. Lecun, Y. Bengio, G. Hinton, Deep Learning, Nature 521 (7553) (2015) 436–444.
[39] Y. Zheng, Q. Liu, E.H. Chen, Y. Ge, J.L. Zhao, Time series classification using multi-channels deep convolutional neural networks, Web-Age Information Management (2014) 298–310.
[40] B. Xu, N.Y. Wang, T.Q. Chen, M. Li, Empirical Evaluation of Rectified Activations in Convolutional, Network (2015). https://arxiv.org/pdf/1505.00853.
[41] S. Ioffe, C. Szegedy, Batch Normalization: Accelerating Deep Network Training by Reducing Internal Covariate Shift, 2015. https://arxiv.org/abs/1502.03167.
[42] S. Ruder, An overview of gradient descent optimization algorithms, 2017. https://arxiv.org/abs/1609.04747.
[43] W.C. Hsu, T. Sugiarto, J.W. Chen, Y.J. Lin, The design and application of simplified insole-based prototypes with plantar pressure measurement for fast screening of flat-foot, Sensors 18 (11) (2018) 1–14.
[44] O.S. Schneider, K.E. MacLean, K. Altun, I. Karuei, M.M. Wu, Real-time gait classification for persuasive smartphone apps: structuring the literature and pushing the limits, IUI 2019 (2019) 19–22.
[45] J.W. Han, M. Kamber, J. Pei, Data Mining: Concepts and Techniques, third ed., Morgan Kaufmann, MA, USA, 2011.
[46] V. Vapnik, The Nature of Statistical Learning Theory, Springer-Verlag, New York, NY, USA, 2000.
[47] N.U. Ahamed, D. Kobsar, L.C. Benson, C.A. Clermont, S.T. Osisc, R. Ferber, Subject-specific and group-based running pattern classification using a single wearable sensor, J. Biomech. 84 (2019) 227–233.
[48] J.A. Ramirez-Bautista, J.A. Huerta-Ruelas, L.T. Kóczy, M.F. Hatwágner, S.L. Chaparro-Cárdenas, A. Hernández-Zavala, Classification of plantar foot alterations by fuzzy cognitive maps against multi-layer perceptron neural network, Biocybern. Biomed. Eng. 40 (1) (2020) 404–414.
[49] F. Horst, S. Lapuschkin, W. Samek, K.R. Müller, W.I. Schöllhorn, Explaining the Unique Nature of Individual Gait Patterns with Deep Learning, Sci. Rep. 9 (2391) (2019).